Correlation function diagnostics for type-I fracton phases

Trithep Devakul,[1] S. A. Parameswaran,[2,*] and S. L. Sondhi[1]

[1] *Department of Physics, Princeton University, Princeton NJ 08540, USA*
[2] *The Rudolf Peierls Centre for Theoretical Physics, University of Oxford, Oxford OX1 3NP, UK*

Fracton phases are recent entrants to the roster of topological phases in three dimensions. They are characterized by subextensively divergent topological degeneracy and excitations that are constrained to move along lower dimensional subspaces, including the eponymous fractons that are immobile in isolation. We develop correlation function diagnostics to characterize Type I fracton phases which build on their exhibiting *partial deconfinement*. These are inspired by similar diagnostics from standard gauge theories and utilize a generalized gauging procedure that links fracton phases to classical Ising models with subsystem symmetries. En route, we explicitly construct the spacetime partition function for the plaquette Ising model which, under such gauging, maps into the X-cube fracton topological phase. We numerically verify our results for this model via Monte Carlo calculations.

Introduction.—Recent studies[1–7] of exactly-solvable stabilizer codes in three dimensions have identified a new class of topologically ordered states that exhibit subextensive topological degeneracy on closed manifolds. Unlike the emergent gauge theories of topological order these "fracton" models lack a point-like excitation free to propagate in 3D. Owing to this, they exhibit translationally-invariant glassy dynamics even at nonzero energy density[8,9]. Instead of fully deconfined point particles, their excitation spectrum generically includes immobile "fractons", as well as a hierarchy of other excitations free to move along lower-dimensional subspaces. Depending on whether fractons may be created at the corners of two-dimensional membranes, or only upon the application of fractal operators, fracton models may be further divided into 'Type I' or 'Type II' fracton phases, in turn related to distinct subsystem symmetries of the classical spin models related to them via a generalized gauging procedure[6,7]. Finally we note that resonating plaquette phases as discussed in Ref. 10–12 have the potential to describe fracton phases.

Despite rapid progress[13–25] in advancing the theory of these novel 3D topological phases, there is a paucity of sharp characterizations of fracton deconfinement away from the stabilizer limit, e.g. when fractons acquire dynamics or are at finite density. One possible diagnostic is to extract topological contributions to the entanglement entropy[26–28], but this requires an exact computation of ground states, typically challenging in 3D, and does not immediately generalize to $T > 0$. For topological orders described by standard lattice gauge theories, a trio of loop observables suitably oriented in Euclidean space-time serves this role, and furthermore may be directly computed from, e.g. quantum Monte Carlo simulations. Can such diagnostics be adapted to study these new states in the presence of dynamical fractonic matter?

Here, we answer this in the affirmative for the so-called X-cube model, and argue that our results may be generalized to all Type-I fracton phases of which it is the paradigmatic example. We do so by formulating a generalized "plaquette gauge theory" (PGT) for the plaquette Ising model, a classical spin model with spin-flip symmetries along planar subsystems. The PGT (and its dual, which we will introduce) describes a perturbed X-cube model. Although quasiparticle excitations of these models are always constrained to lower-dimensional subspaces and are hence not truly deconfined, they are in a sense *partially* deconfined within these subspaces. We show that the standard technology for diagnosing the deconfined and confined phases[29,30], reviewed next, can indeed be generalized in a straightforward manner to detect this partial deconfinement that can be viewed as a defining property of fractonic matter.

Ising Gauge Theory.— To orient our discussion, we first review the gauging procedure that leads to the Ising gauge theory (IGT), and discuss its deconfinement diagnostics[29]. We begin with the classical Ising Hamiltonian on the square lattice, with matter degrees of freedom τ_s^z on the site s, and nearest-neighbor $J\tau^z\tau^z$ interactions (we will often suppress the site subscript when the meaning is obvious). This model has a global $\mathbb{Z}_2$ symmetry, which is a flip of all τ^z, that can be 'gauged' by introducing an Ising spin σ_l^z on each link l, and modifying the interaction term accordingly: $J\tau^z\tau^z \to J\sigma^z\tau^z\tau^z$. This expands the global Ising symmetry to a local $\mathbb{Z}_2$ gauge symmetry G_s on each site, obtained by considering a simultaneous flip of τ_s^z and each σ^z coupled to it by an interaction term — i.e., those on the 4 links surrounding site s. The IGT is obtained by restricting to the subspace where $G_s = +1$ for all s. Finally, we give quantum dynamics to both gauge and matter degrees of freedom by adding terms $\Gamma\sigma^x$ and $\Gamma_M\tau^x$ to our Hamiltonian. To complete our construction of the IGT Hamiltonian, we add a gauge 'potential energy' by identifying the simplest gauge-invariant pure-σ^z term that commutes with τ^x, here a product of σ^z around a plaquette p, with coupling strength K, yielding

$$\begin{aligned}\mathcal{H}_{\text{IGT}} \;=\; & -K\sum_p \prod_{l\in\partial p}\sigma_l^z - \Gamma_M\sum_s \tau_s^x \\ & -J\sum_l \sigma_l^z \prod_{s\in\partial l}\tau_s^z - \Gamma\sum_l \sigma_l^x\end{aligned} \tag{1}$$

subject to the constraint $G_s = \tau_s^x\prod_{l\in\partial s}\sigma_l^x = 1$, where

s, l, p denote links, sites, and plaquettes, and we denote by $\partial s, \partial l, \partial p$ the objects touching them (in this case the 4 links surrounding a site, the 2 sites straddling a link, and the 4 links encircling a plaquette).

Precisely at $J = \Gamma = 0$, this model reduces to Kitaev's Toric code[31] (this can be seen by enforcing the constraint to replace τ^x_s by $\prod_{l\in\partial s}\sigma^x_l$). Introducing nonzero J or Γ can then be thought of as perturbations from the Toric code point. Turning Γ too high will drive the gauge theory into a trivial confined phase, and turning J too high will result in a Higgs transition into a symmetry broken phase where $\langle\tau^z\rangle$ obtains an expectation value. These two limits are smoothly connected[32], thus we will refer to both as the confined limits, and small perturbations of the Toric code point as the deconfined limit (characterized by $\mathbb{Z}_2$ topological order).

Let us now consider moving along the "pure gauge theory" axis, $\Gamma > 0, J = 0$, along which the matter is static, $\tau^x_s = 1$ and therefore can be ignored. Here, the spatial Wilson loop, $W = \prod_{l\in C}\sigma^z_l$, where C is a closed loop (taken for simplicity to be an $L \times L$ square), serves as a diagnostic that can distinguish the confined and deconfined phases. At the Toric code point $\Gamma = 0$, we have $\langle W\rangle = 1$. Small perturbations in Γ create local fluctuations of pairs of "visons", plaquettes on which $\prod_{l\in\partial p}\sigma^z_l = -1$ (the magnetic flux excitations of the theory). As the Wilson loop measures the average parity of visons contained within it, these fluctuations will cause the expectation value to decay proportionally to the perimeter of the loop, following a perimeter law: $\log\langle W\rangle \sim -L$ for large L. In the confined phase at large Γ, the visons are condensed and so here $\log\langle W\rangle \sim -L^2$ follows an *area* law for large L. However, as soon as we add dynamical matter $J > 0$, the Wilson loop follows a perimeter law *everywhere*. To see this, notice that in perturbation theory in J about the $J = 0$ ground state $|\psi_0\rangle$, a term matching the Wilson loop operator appears at $O(J^L)$: $|\psi\rangle = |\psi_0\rangle + \alpha e^{-\beta L} W|\psi_0\rangle + \dots$ for some numbers $\alpha \sim O(1)$ and $\beta \sim -\ln J$, so that there is at least a perimeter law component to $\langle W\rangle$ which dominates as $L \to \infty$. Thus, the Wilson loop fails as a deconfinement diagnostic as soon as $J > 0$.

Now, consider moving along the "pure matter theory" axis, with $J > 0, \Gamma = 0$. Here, the gauge field exhibits no fluctuations, and it is convenient to work with $\sigma^z = 1$, and project onto the gauge invariant subspace if needed. In this subspace, the Hamiltonian is simply the original Ising model, in a transverse field. Beyond a critical J, there is a transition to an ordered phase where $\langle\tau^z\rangle$ gains an expectation value. However, τ^z alone does not correspond to a gauge invariant operator; only pairs of τ^z do. This transition can therefore be diagnosed by an *open* Wilson loop $\tau^z_s\tau^z_{s'}\prod_{l\in C_{ss'}}\sigma^z_l$ where $C_{ss'}$ is a path connecting sites s and s', which in this subspace is simply the spin-spin correlation function $\langle\tau^z_s\tau^z_{s'}\rangle$. As one takes $|s - s'| \to \infty$, this either goes to zero in the deconfined (paramagnetic) phase, or approaches a constant in the confined (Higgs ferromagnetic) phase. This can also be understood without referring to the matter theory as the vanishing of a line-tension in the Euclidean action[29]. Now consider adding in a small Γ perturbatively: σ^x anticommutes with the σ^z chain, and so $\langle\tau^z_s\sigma^z\dots\sigma^z\tau^z_{s'}\rangle$ decays to zero exponentially with $|s - s'|$ in both phases. We therefore again are in a situation where a diagnostic that works exactly along this axis fails as soon as $\Gamma > 0$.

How then can we distinguish the confined from the deconfined phase away from these special axes? The answer is to measure an appropriate line tension, using wisdom gained from the Euclidean path integral representation which maps the problem on to an isotropic 3D statistical mechanical problem of edges and surfaces[29,33]. This can be linked to the expectation value of a "horseshoe operator", viz. an $L \times L$ Wilson loop cut in half (with τ^z inserted at the ends for gauge invariance), $W_{1/2} = \tau^z_s\tau^z_{s'}\prod_{l\in C_{1/2}}\sigma^z_l$, where $C_{1/2}$ defines the half-Wilson loop of dimension $L/2 \times L$, terminating at sites s and s'. The ratio of expectation values as $L \to \infty$,

$$\mathcal{R}(L) = \frac{\langle W_{1/2}\rangle}{\sqrt{\langle W\rangle}} \xrightarrow{L\to\infty} \begin{cases} 0 & \text{deconfined} \\ \text{const.} & \text{confined} \end{cases} \tag{2}$$

can then be understood as measuring the "cost" of opening the Wilson loop. In the deconfined phase, opening a Wilson loop will cause the expectation value to decay exponentially with the size of the gap. In the confined phase, the expectation value of the Wilson loop follows a perimeter law regardless of whether it is opened or closed, thus the scaling with L is exactly cancelled out by dividing by the square root of the full Wilson loop.

Since the Euclideanized IGT is space-time symmetric, by choosing distinct orientations and 'cuts' of the loop, we can identify three different diagnostics. Besides (1) the 'spatial loop' discussed above, the two possible cuts for the orientation extending along the time direction also have elegant physical interpretations[29]: either (2) as the Fredenhagen-Marcu diagnostic[34,35], measuring the overlap between the ground state and the normalized two-spinon state; or (3) as a measure of delocalized spinon (electric-charge) excitations. By the self-duality of the IGT this exercise could have been done in the dual model, which defines a different Wilson loop object and exactly interchanges the role of the gauge (Γ, K) and matter (J, Γ_M) sectors[36].

Euclidean Path Integral and Wilson Loops for Plaquette Gauge Theory .— We will now proceed with our analysis of the "plaquette gauge theory" (PGT), which arises from applying the generalized gauging procedure to the classical plaquette Ising model[6,7,38] and produces X-cube fracton topological order in its deconfined phase, by analogy with the IGT of the preceding section. The main deviation from the standard gauging procedure is that we place σ at the center of each interaction in the Hamiltonian (the plaquettes in this model), rather than always on the links (these are the "nexus" spins of Ref. 6).

The classical (3D) plaquette Ising model (CPIM) is described by $\mathcal{H}_{\text{CPIM}} = -J\sum_p\prod_{s\in\partial p}\tau^z_s$, where the sum is

over plaquettes and the product is over the four sites at the corner of plaquette p. Applying the gauging procedure, we arrive at the PGT Hamiltonian,

$$\begin{aligned}\mathcal{H}_{\rm PGT} &= -K\sum_{c,i}\prod_{p\in b_i(c)}\sigma_p^z - \Gamma_M\sum_s \tau_s^x \\ &\quad -J\sum_p \sigma_p^z\prod_{s\in\partial p}\tau_s^z - \Gamma\sum_p\sigma_p^x\end{aligned} \tag{3}$$

where now the σs live at the center of plaquettes p, c denotes a cube, and $b_i(c)$ for $i=1,2,3$ correspond to the three distinct combinations of four plaquettes that wrap around the cube c (sometimes aptly called "matchboxes"). We further have a constraint defined on each site s, $G_s=\tau_s^x\prod_{p\in\partial s}\sigma_p^x=1$, where the product is over the 12 plaquettes touching s. Note that this model, for small J and Γ, is just a perturbed X-cube model (which is usually defined on the *dual* lattice where our plaquettes become links) and that the topological order is stable to small perturbations[41]. The deconfined phase of this model hosts two types of excitations: the "electric" ($\tau^x=-1$) excitations are fractons, while the "magnetic" excitations are one-dimensionally mobile quasiparticles, which we will refer to as lineons (short for "line vison").

In standard gauge theory, one is often only concerned about the deconfinement of the electric charge excitations. The X-cube model (unlike the Toric code) does not possess an electro-magnetic ($\sigma^z\leftrightarrow\sigma^x$) self-duality, so for completeness we also consider the "electromagnetic" *dual* to the PGT. This dual model arises naturally from the same generalized gauging procedure on the *classical* dual of the CPIM, which can be written as an anisotropically coupled Ashkin-Teller model[39,40]. Note that the duality discussed here maps between two full gauge-matter theories; the "F-S duality" between a pure matter theory and pure fracton gauge theory[6] is a limiting case. We construct deconfinement diagnostics for the electric charge in both the PGT and its dual, thus providing diagnostics for both fracton and lineon excitations.

For a full space-time discussion of Wilson loop analogues, we construct a discrete-time Euclidean path integral for the PGT Hamiltonian Eq. (3) via the usual Suzuki-Trotter decomposition. The gauge constraint is enforced by the introduction of auxiliary spin-1/2 degrees of freedom along the time-links of the 4D hypercubic lattice[36,37], that we will denote λ (in the IGT one has a space-time symmetric structure so these spins can be thought of as σ spins along the time-links, but this is not the case here). After a straightforward calculation (for details, see[42]), we find $Z_{\rm PGT}=\mathrm{Tr}_{\{\tau,\sigma,\lambda\}}e^{-\mathcal{S}_{\rm PGT}}$, with the Euclidean action

$$\begin{aligned}\mathcal{S}_{\rm PGT} &= -\tilde{K}\sum_{t,c,i}\prod_{p\in b_i(c)}\sigma_p^{(t)} - \tilde{\Gamma}_M\sum_{t,s}\tau_s^{(t)}\lambda_s^{(t)}\tau_s^{(t+1)} \\ &\quad -\tilde{J}\sum_{t,p}\sigma_p^{(t)}\prod_{s\in\partial p}\tau_s^{(t)} - \tilde{\Gamma}\sum_{t,p}\sigma_p^{(t)}\sigma_p^{(t+1)}\prod_{s\in\partial p}\lambda_s^{(t)}\end{aligned} \tag{4}$$

where the integer t labels the Euclidean time slice (which extends to infinity for zero temperature), $\tau_s^{(t)}$ ($\sigma_l^{(t)}$) is now a classical Ising variable associated with sites (links) in the time slice t, and $\lambda_s^{(t)}$ is similarly associated with the link connecting site s between time slices t and $t+1$. The couplings in $\mathcal{S}_{\rm PGT}$ are related to those in $\mathcal{H}_{\rm PGT}$ and the Trotter time step ϵ via $\tilde{K}=\epsilon K$, $\tilde{J}=\epsilon J$, and $\tilde{\Gamma}_{(M)}=-\frac{1}{2}\log\tanh\epsilon\Gamma_{(M)}$. This can be viewed as a statistical mechanical model of edges, surfaces, and volumes in 4D, but with a more subtle set of rules for how to build allowed objects from these.

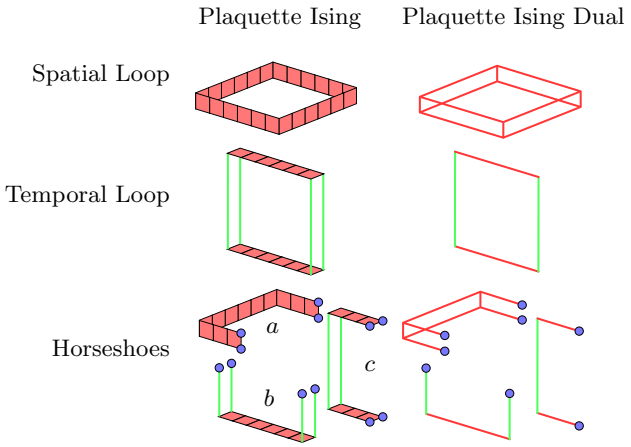

FIG. 1: The Euclidean time representation of the Wilson loop and horseshoe generalizations for the PGT and its dual, which realize the X-cube topological phase. Blue circles represents τ (which lie on vertices), red represent σ (which lie on the spatial plaquettes in the PGT, but on spatial links in its dual), and green lines represent the auxiliary spin λ (which lie on the links along the imaginary time direction). Non-equal time operators are shown projected to a 2+1D subspace, with the time direction pointing "up" in the page. The three possible cut orientations are labeled by a,b, and c.

Proceeding by analogy with the IGT, we construct the Wilson loops for the PGT and its dual (Fig. 1). Spatial loops are constructed by choosing a set of cubes c whose centers lie in a plane and taking the product of their 'matchbox' terms (terms multiplying K in the action) such that the vacant squares of each matchbox lie parallel to the plane, resulting in a 'ribbon loop' encircling it. This can equivalently can be thought of as the dynamical process of moving a two-dimensionally mobile combination of charges around in a loop lying in a plane, via applications of the term multiplying J in the action. For the PGT, this is a pair of fractons, while for the dual it is a pair of parallel-moving lineons. Temporal Wilson loops are constructed in a similar fashion, by taking the product of the six-spin terms (that multiply Γ) corresponding to each space-time cube in an $L\times L_\tau$ spacetime sheet, leaving open spatial ribbons at the initial and final slices, whose corners are linked by strings of λs. This can equivalently be constructed by moving a *one*-dimensionally mobile combination of charges a distance L apart, evolving both for L_τ in imaginary time,

and bringing them back together again. The combination again consists of a fracton-pair in the PGT, but now only a single lineon in the dual. The corresponding horseshoes (or cut Wilson loop) operators are then obtained by cutting open the loop and terminating it with appropriate combination of τs, with three distinct possible orientations labeled a, b, and c in Fig. 1.

Diagnostic behaviors.— We now consider the expectation value of these operators at various points in the phase diagram. First, note that the spatial Wilson loop alone functions as a diagnostic only in the pure gauge theory. When $J = 0$, for small Γ, vison-pair fluctuations occur only on small length scales, so that only pairs along the perimeter of the loop will affect the expectation value. In contrast, flux excitations are condensed in the confined phase at large Γ, so that the loop now exhibits an area law. As in the IGT, for any $J > 0$ the loop obeys a perimeter law in both phases.

Next, notice also that the spatial horseshoe alone serves as a diagnostic only along the $\Gamma = 0$ axis, where it can be understood as measuring the vanishing of a macroscopic string tension. To understand why this expectation value is nonzero in the Higgs/confined phase, we draw on known results for the CPIM[38]. Early work on the "fuki-nuke" model[44], which may be thought of as an anisotropic limit of the CPIM with $J = 0$ for the plaquettes in the xy plane, reveals that this model maps on to a stack of decoupled 2D (xy-planar) Ising models. In terms of the original spins, the local observable $\langle \tau^z_s \tau^z_{s+\hat{z}} \rangle$ gains a nonzero expectation value in the ordered phase, but is free to spontaneously break the symmetry in different directions for each xy plane. Now, the horseshoe operator (a) obtained by cutting open a xy Wilson loop is exactly the correlation function of this observable: $\langle \tau^z_s \tau^z_{s+\hat{z}} \tau^z_{s'} \tau^z_{s'+\hat{z}} \rangle$ for s,s' which are constrained to be in the same xy plane, which therefore approaches a constant as $|s - s'| \to \infty$ in the ordered phase. This correlator continues to function as a diagnostic even for the isotropic model, where we are free to choose planes oriented in any direction[43,45,46].

Away from the $J = 0$ or $\Gamma = 0$ cases, we must rely on the ratios $\mathcal{R}(L)$ (Eq. (2)) to distinguish between the confined and (partially) deconfined phases. The ratio for the spatial cut (a in Fig. 1) as before measures of the cost of opening up a gap in the loop, which depends exponentially on the size of the gap in the deconfined phase, but not in the confined phase. In the supplementary material[42], we verify numerically using quantum Monte Carlo that $\mathcal{R}(L)$ shows the expected behavior crossing the transition at a generic point in the phase diagram. At $\Gamma = 0$, $\mathcal{R}(L)$ reduces to the "fuki-nuke" correlation function above.

Next, we examine the temporal loops. Consider the cut b of the PGT, $W_{1/2} = \tau^z_s \tau^z_{s+u} \tau^z_{s'} \tau^z_{s'+u} \prod_{p \in C^u_{ss'}} \sigma^z_p(-T/2)$, where s,s' are two sites on the same plane orthogonal to $u = \hat{x}, \hat{y}, \hat{z}$, and $C^u_{ll'}$ defines the set of plaquettes forming a path between them (as in Figure 1). We have also defined $\sigma^z(T) = e^{\mathcal{H}T} \sigma^z e^{-\mathcal{H}T}$, and $T = L/c$ for a velocity c in the continuum time limit $\epsilon \to 0$. Calling our candidate two-fracton-pair (4 fractons in total) state $|\chi\rangle = W_{1/2}|G\rangle$, created from the ground state $|G\rangle$, we see that $\mathcal{R}(L) = \langle G|\chi\rangle / \sqrt{\langle \chi|\chi\rangle}$ measures the overlap between the ground state and our candidate state. This is a generalization of the Fredenhagen-Marcu diagnostic[34,35] measuring the deconfinement of fracton-pairs, with the constraint that the two fracton-pairs must be in the same plane of movement. The final orientation of the horseshoe (cut c) probes the existence of delocalized fracton-pair states in the spectrum, in exactly the same way as the delocalized spinons are probed the IGT[29].

Thus, rather than measuring the deconfinement of single spinons as in the IGT, our Wilson loop and horseshoe generalizations instead measure the same quantities but for the smallest mobile combinations of quasiparticles in their subspace of allowed movement. For the PGT, this is a fracton-pair. As stated, these diagnostics only probe the deconfinement properties of fracton-*pairs*, and not single fractons. To identify the deconfinement of individual fractons one can do the same calculation but using Wilson loops and horseshoes with a finite width that also scale with L. This distinction can be important, for example, in an anisotropic version of the PGT[42] which exhibits an intermediate phase in which single fractons are confined into pairs, while pairs remain deconfined (reminiscent of quark confinement into mesons).

Concluding Remarks.— We have shown that deconfinement diagnostics for the Ising gauge theory (or conventional topological order) can be generalized to the plaquette Ising gauge theory, which exhibits the X-cube fracton topological order in its deconfined phase. Despite never being fully deconfined in the sense of having excitations free to move in all three dimensions, the expectation value of our generalized Wilson loops and horseshoes diagnoses the *partial* deconfinement of these excitations, with various physical interpretations depending on their orientation in Euclidean space-time. The procedure for identifying Wilson loop type operators is quite general, and can be extended to other similar type-I fracton models, such as the checkerboard model[6]. However, the extension to type-II fracton theories where the fractons (and their composites) are fully immobile remains an open question worthy of future study.

Acknowledgments

We thank Rahul Nandkishore for discussions and comments on the draft. This work was supported by DOE Grant No. DE-SC/0016244 (SLS).

[*] On leave from: Department of Physics and Astronomy, University of California Irvine, Irvine CA 92617, USA.

[1] C. Chamon, Phys. Rev. Lett. **94**, 040402 (2005).

[2] J. Haah, Phys. Rev. A **83**, 042330 (2011).

[3] S. Bravyi, B. Leemhuis, and B. Terhal, Ann. Phys. **326**, 839 (2011).

[4] Beni Yoshida, Phys. Rev. B **88**, 125122 (2013).

[5] S. Vijay, J. Haah, and L. Fu, Phys. Rev. B **92**, 235136 (2015).

[6] S. Vijay, J. Haah, and L. Fu, Phys. Rev. B **94**, 235157 (2016).

[7] D. J. Williamson, Phys. Rev. B **94**, 155128 (2016).

[8] I. H. Kim and J. Haah Phys. Rev. Lett. **116**, 027202 (2016)

[9] A. Prem, J. Haah, R.M. Nandkishore, Phys. Rev. B **95**, 155133 (2017)

[10] S. Pankov, R. Moessner, S. L. Sondhi, Phys. Rev. B **76**, 104436 (2007).

[11] Cenke Xu and Congjun Wu, Phys. Rev. B **77**, 134449 (2008).

[12] T. Devakul, arXiv:1712.05377 (2017).

[13] M. Pretko,Phys. Rev. B **95**, 115139 (2017).

[14] M. Pretko, Phys. Rev. B **96**, 035119 (2017).

[15] M. Pretko, Phys. Rev. D **96**, 024051 (2017).

[16] M. Pretko, Phys. Rev. B **96**, 115102 (2017).

[17] M. Pretko, arXiv:1707.03838.

[18] S. Vijay, arXiv:1701.00762.

[19] H. Ma, E. Lake, X. Chen, M. Hermele, Phys. Rev. B **95**, 245126 (2017).

[20] K. Slagle and Y.-B. Kim, arXiv:1704.03870.

[21] K. Slagle and Y.-B. Kim, arXiv:1708.04619.

[22] G. B. Halász, T. H. Hsieh, arXiv:1703.02973.

[23] G. B. Halász, T. H. Hsieh, L. Balents, arXiv:1707.02308.

[24] A. Prem, M. Pretko, R. Nandkishore, arXiv:1709.09673.

[25] O. Petrova, N. Regnault, arXiv:1709.10094.

[26] B. Shi and Y.-M. Lu, arXiv:1705.09300.

[27] H. Ma, A.T. Schmitz, S.A. Parameswaran, M. Hermele, and R.M. Nandkishore, arXiv:1710.01744 (2017).

[28] A.T. Schmitz, H. Ma, R.M. Nandkishore, and S.A. Parameswaran, arXiv:1712.02375 (2017).

[29] K. Gregor, D. A. Huse, R. Moessner, S. L. Sondhi, New J.Phys.**13**:025009, 2011.

[30] A. Chandran, F. J. Burnell, V. Khemani, S. L. Sondhi, J. Phys.: Condens. Matter **25** (2013) 404214.

[31] A. Yu. Kitaev, Annals of Physics **303**, 2 (2003).

[32] E. Fradkin, S. H. Shenker, Phys. Rev. D **19**, 3682 (1979).

[33] D. A. Huse and S. Leibler, Phys. Rev. Lett. **66**, 437 (1991).

[34] K. Fredenhagen, M. Marcu, Phys. Rev. Lett. **56**, 223 (1986).

[35] K. Fredenhagen, M. Marcu, Nucl. Phys. Proc. Suppl. **4**, 352 (1988).

[36] J. B. Kogut, Rev. Mod. Phys. **51**, 659 (1979).

[37] R. Moessner, S. L. Sondhi, and Eduardo Fradkin, Phys. Rev. B **65**, 024504 (2001).

[38] D. A. Johnston, M. Mueller, and W. Janke, Eur. Phys. J. Special Topics **226**, 749764 (2017).

[39] D.A. Johnston, R.P.K.C.M. Ranasinghe, J. Phys. A: Math. Theor. **44**, 295004 (2011).

[40] J. Ashkin and E. Teller, Phys. Rev.**64** (1943) 178.

[41] S. Bravyi, M. Hastings, S. Michalakis, J. Math. Phys. **51** 093512 (2010).

[42] See supplementary material for the (i) path integral formulation of the PGT, (ii) an anisotropic version of the PGT, and (iii) numerical verification and phase diagram of the PGT via quantum Monte Carlo.

[43] D. A. Johnston, J. Phys. A: Math. Theor. **45**, 405001 (2012).

[44] M. Suzuki, Phys. Rev. Lett. **28**, 507 (1972).

[45] Y. Hashizume, M. Suzuki, Int. J. Mod. Phys. B **25**, 73 (2011).

[46] Y. Hashizume, M. Suzuki, Int. J. Mod. Phys. B **25**, 3529 (2011).